Paper No. 1683. (quote when citing this article)
Eleventh World Conference on Earthquake Engineering
ISBN: 0 08 042822 3

SOFT SOIL RESPONSE OF A BRIDGE PIER

DR. SOHAIL M. QURESHI, and DR. T. MASOOD

NIT, National University of Sciences and
Technology, Pakistan, and Nespak, Lahore, Pakistan.

ABSTRACT

This research was initiated to access the failure characteristics of bridge piers. The main objective was to carry out an experimental evaluation of such failures. A bridge pier model was constructed and tested for a fixed base response and a flexible, soft soil response. The results showed a strong nonlinear response for the fixed structure and a softening of the hard spring under increased dynamic excitation. The additive effect of the soft soil was to render the response almost linear for large amplitudes, but strongly nonlinear characteristics at small input accelerations. A lumped parametric approach was considered sufficient to evaluate the soil properties. Analytical interpretations became necessary to evaluate the dynamic material properties experimentally, and a need for the explanation of the nonlinear failure phenomenon, using equivalent linearization for system identification.

KEYWORDS

Inelastic response; bridge pier; soft soil; soil-structure interaction.

INTRODUCTION

Earthquakes are known to cause severe structural damage and a more realistic design would permit yielding, resulting in energy absorption or dissipation such that the structure is better able to withstand severe earthquake excitations. A reinforced concrete pier was constructed (fig. 1) for an oscillator response evaluation. The model is $2.80m$ high, top to bottom, with a circular footing of $1.60m$ diameter and $0.55m$ depth; the top cantilevers were $2.00m$ either side and tapered. The model had $30mm$ diameter holes for the placement of the oscillator and $50mm$ holes ($4No.$) in the foundation for base fixity. Rapid hardening cement concrete with a 3 day compressive strength of 234 Kg/cm^2 was used in the construction. A main reinforcement of $D16$ was used in the column and the top girder respectively with $D13$ being used in the footing. A distribution steel of $D10$ was used throughout.

The instrumentation consisted of a $VE3-7$ type oscillator with a $400Kg$ dead weight and a pen oscillograph of $8K22-2-H$ type. Figure 1 shows details of the strain gauge arrangement. A total of 12 strain gauges $S1$ to $S12$ were attached to the main reinforcement at the base of the column for direct strain measurement with a portable $DPM-6H$ type strain recorder.

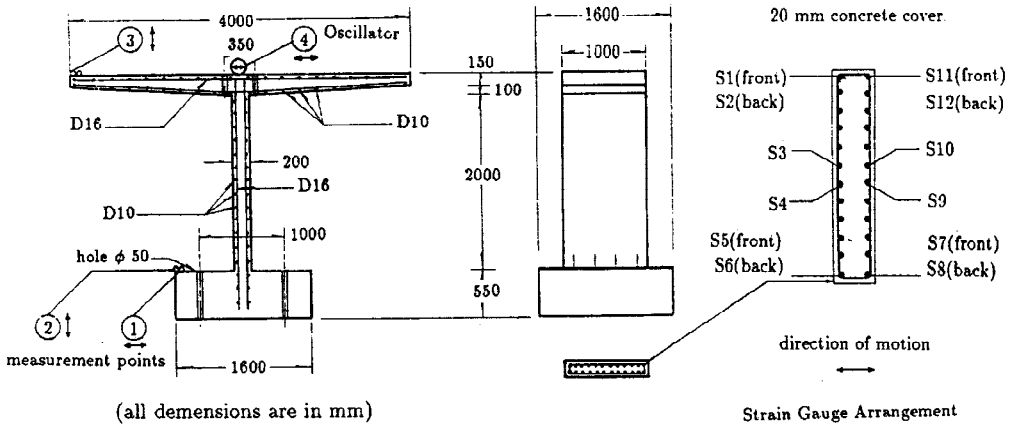

Fig. 1

Table 1 Experimental sequence

TEST	Support Fixity Condition	Counter Weight No.	Frequency (*Hz*)	P (*N*)	Acc. (*gal*)
I	Flexible	5	2.58	101	34
		10	2.38	173	65
		30	2.14	416	142
		90	2.07	1080	272
II	Fixed	5	4.33	284	329
		10	3.86	455	407
		20	3.34	679	727
		30	3.26	967	752
		40	3.04	1110	1030
		50	2.93	1280	1600
III	Flexible	10	2.07	131	49
		30	1.84	305	117
		90	1.58	633	224
IV	Fixed	60	2.80	1380	1350
		70	2.70	1480	1240
		80	2.63	1580	1290
V	Flexible	10	1.93	113	40
		30	1.74	275	87
		90	1.53	594	230

The test specimen was subjected to nine increasing periodic loadings detailed in Table 1 and frequency response (accelerations, displacements and strains) was measured at the first resonant frequency and at 0.1 Hz intervals. After testing frequency reponse curves were drawn (Fig. 2) for the test loadings. The experimental sequence is detailed below. The pier was tested on flexible foundation for the 5, 10, 30, and 90 loads as Test I. The Test II was on fixed base for the 5, 10, 20, 30, 40, and 50 loads. The Test III was again on the flexible foundation for the loads 10, 30, and 90. The Test IV was on a fixed base for the 60, 70, and 80 loads. This was finally followed by the Test V on the flexible foundation for the 10, 30, and 90 loads. The interpretation of these Tests 1~5 could only be done, if an identification of the parameters for each test is done separately. The tests I, II and V on flexible foundation show a linear response with increased loading due to the additive effect of 1) the soft soil spring, 2) the hard spring resulting from concrete nonlinearity and crack

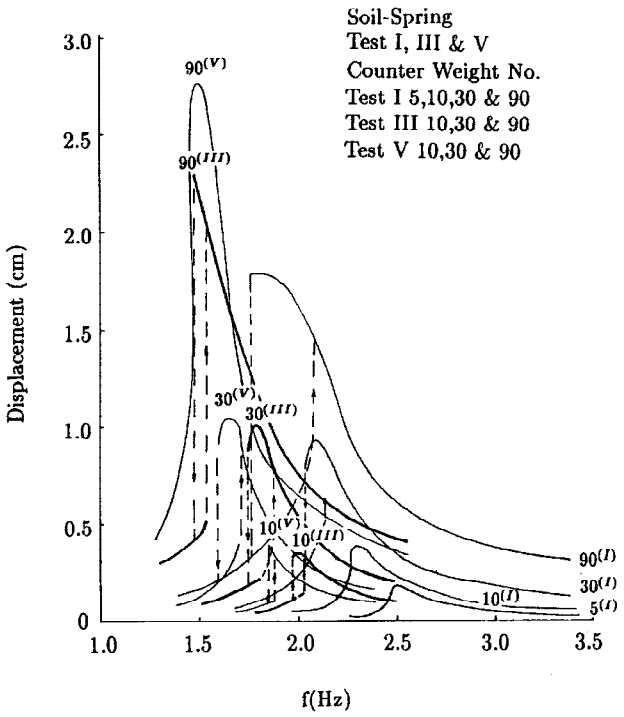

Fig. 2

growth, and 3) the bond-slip resulting in pinching behaviour. The frequency response curves for Test II and IV show a continuous increase in the displacement and acceleration response up till periodic load 50 and thereafter a reduction in the maximum displacement and acceleration response. The damping coefficient was calculated for each load using the half-power method. It is also evident from the response curves that the damping during increasing frequency was less than during decreasing frequency, because of the increased energy dissipation due to tension cracks and bond-slip as the stresses increased.

The response curves in Fig. 3 indicate a strong hard spring effect and a progressive softening of this spring with increments in the amplitude of the cyclic loading. At this stage of the experimental evaluation, a simple single degree-of freedom (SDOF) model seemed sufficient to predict the nonlinear properties of the system.

Lumped Plasticity Model

Reinforced Concrete Structures are usually modeled by a lumped plasticity at hinges and a distributed flexibility to account for the spread of plasticity. An empirical parametric approach that can best describe the lumped plasticity can be used to fit the observed experimental data. Two basic characteristics of reinforced concrete structures play an important role in determining response to strong ground motions. They are the changes in (a) stiffness and (b) energy dissipation capacity, and are related to the maximum displacement. A key property of reinforced concrete systems subjected to strong ground motion is the change in effective natural frequency related to the reduction in stiffness caused by cracking and local spalling of the concrete as well as slipping and reduction in effective modulus of the steel. The natural frequency changes noted are consistent with stiffness changes. The initially measured low amplitude frequency corresponds to the pier with virtually intact concrete. Excursions into the inelastic range reduce the effective stiffness of the pier, and its effective natural frequency.

The area within a cycle of the force displacement curve is a critical parameter for dynamic response because it is a measure of energy dissipated by the vibrating system in that cycle. As

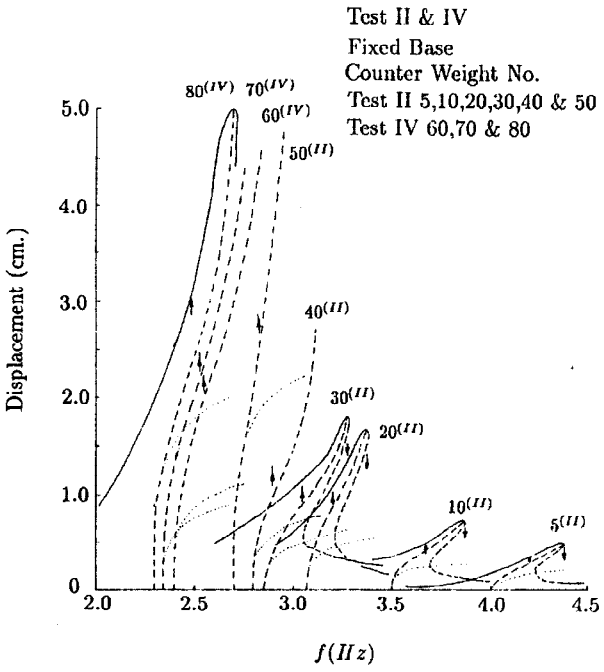

Fig. 3

the pier softened by the displacement beyond cracking, and responded to the remainder of the motion as a system with a lower apparent natural frequency and greater capability to dissipate energy. As the structure is excited to larger displacements, its stiffness decreases and its capacity to dissipate energy increases. Both effects can be related to the displacement attained (interpreted as strain, curvature, rotation or deflection) or, to ductility defined as the ratio of maximum to yield displacement.

Available Ductility and Ductility Demand

The available ductility is determined experimentally or analytically and the required ductility demand is a measure of the severity of the earthquake force on the plastic hinge of the bridge pier. In actual practice, this is a complex phenomenon dependent on the seismic force level, the characteristics of the earthquake, the structural systems paramters, the location of the plastic hinge.

A primary consideration in seismic design specifications is the energy absorbed in plastic hinges that occurs in supporting column members and the local ductility required at a plastic hinge. The plastic hinge occurs over an equivalent plastic hinge length h. If the plastic hinge is assumed equal to the member depth for a column of depth to height ratio of 0.1, the curvature ductility is significantly larger than the displacement ductility for intermediate period range. As the structure is loaded monotonically in the longitudinal direction plastic hinges will form at either the top or the bottom of the columns. The sequence of the formation of the plastic hinges in the columns is dependent on the capacity of the concrete section, the distribution of inertia forces, and the relative stiffness of the connections at the superstructure and the foundations. The sequence of hinge formation in short, stiff columns which may yield initially produces a ductility demand significantly larger than of longer, flexible columns.

Soil Response Analysis

It is widely accepted that the dynamic response of a structure supported on soil is different from the response of a fixed base structure because of two reasons:

1. The flexibly supported structure has more degrees of freedom and hence different dynamic characteristics than a fixed base structure.
2. A large part of the vibration energy is dissipated by radiation of waves into the supporting medium and by damping in the foundation medium.

Simplified formulae using the elastic-half space approach are used in analyses. These formulas were modified to take into account the embedment depth of the circular foundation. The explicit formulas for the stifnesses are :

$$\textit{Vertical} \qquad K_V^0 = \frac{4GR}{1-\nu}$$

$$\textit{Horizontal} \qquad K_H^0 = \frac{8GR}{2-\nu}$$

$$\textit{Rocking} \qquad K_R^0 = \frac{8GR^3}{3(1-\nu)}$$

These formulas represent the static stiffness of a rigid circular foundation of radius R, with G and ν being the shear modulus and Poisson's ratio of the homogenous halfspace. Approximate static stiffnesses as a function of the embedment ratio (E/R) are developed. It is reasonable to assume that the effect of Poisson's ratio on the static stiffnesses is the same for surface foundation as it is for an embedded foundation. In this case polynomial approximations are choosen to account for embedment that depends on embedment parameters only.

$$\textit{Vertical} \qquad K_V^s = K_V^0(1 + 0.54E/R)$$

$$\textit{Horizontal} \qquad K_H^s = K_H^0(1 + E/R)$$

$$\textit{Rocking} \qquad K_R^s = K_R^0(1 + 2.3E/R + 0.58(E/R)^3)$$

Principal Effects of Interaction

The information presented reveals that soil-structure interaction has two principal effects:

1. It decreases the resonant frequency of the system below that of a fixed-base structure, displacing the peak response to the left.
2. It modifies the magnitude of the peak response, decreasing the value for short, squatty structures and increasing the value for tall, slender ones.

An explanation of the second is obviously due to increased rocking of the foundation, the acceleration and the associated inertia forces increase, leading to an increase in the response. Whereas in short structures, response is damped due to stress-wave radiation.

Approximate Model for Soil Response

The replaced single degree of freedom (SDF) oscillator corresponds to the physical model with the spring connected to the base representing the flexibility of the foundation, the spring connected to the mass represents the flexibility of the structure and the dashpot simulates the overall damping of the system. If $w(t)$ represents the total deformation of the replacement oscillator, this deformation must be shared by the two springs in inverse proportion to f^2, whereas the total stiffness of the oscillator is proportional to $\tilde{f}^2$, it follows that the structural deformation, $u(t)$, is related to the total deformation, $w(t)$, by :

$$u(t) = \{\frac{\tilde{f}}{f}\}^2 w(t)$$

The undamped natural frequency of the replacement SDF oscillator, $\tilde{f}$, may be determined from the well known formula

$$\tilde{f} = \frac{1}{2\pi}\sqrt{\frac{g}{\delta_{st}}}$$

where g is the gravitational acceleration and δ_{st} is the deflection of the mass of the superstructure, m, produced by a horizontal force of magnitude mg applied to the mass. δ_{st} is given by

$$\delta_{st} = [\frac{1}{K} + \frac{1}{K_x} + \frac{1}{K_\theta}\frac{h^2}{r^2}]mg$$

where the first term is the structural deformation and the second and third terms represent the effects of the foundation translation and rotation, respectively. The foundation mass and the rotatory inertia of the structural mass are assumed to be negligible. It is evident that the rotational flexibility of the foundation contributes more to δ_{st} than does the translational flexibility when $h/r \geq 1$. Thus, the rotation of the foundation is the most imporatnt factor in lowering the resonant frequency of a tall, slender pier like structure.

METHODS AND COMPARISONS

Fixed Base Tests

In explaining the response curves in Fig. 3 and the actual experimental results, we can conclude that the displacement response increases till the ultimate design capacity of the specimen is reached. The softening of the hard spring is due to the dowel action and bond-slip of the concrete and increases with increase in micro cracks till load 50 is reached in the Test II. At this stage of the experiment, the specimen is induced with the maximum displacement and a maximum acceleration response. This in comparison with the damping coefficient would strengthen our conclusion of increased micro cracking, and an increased damping from load 5 to load 30 and a reduction in the stiffness of the specimen. The damping coefficient at load 50 dips suddenly due to a crack opening and possible start of the separation of concrete from the reinforcement, but a maximum response is indicated prior to structural failure. The progressive response curves after load 50 show an irregular shape and a reduced acceleration and displacement response; but an increase in the damping coefficient. This could be possibly due to the cracks closing on one side of the column. The irregular response curves are because of the separation of concrete and steel, with each one showing a distinct hump in the frequency response curve. Another reason is the presence of higher harmonics in the response curves beyond load 50 is also evident.

The pier was first modeled as a SDOF system with the girder mass and 0.234 of the pier mass lumped at the top of the pier spring. This model was applied with the oscillator load and accelerations were calculated. Although the load varied between 29.0 kg. and 162.0 kg. it produced accelerations varying between 329.0 gal and 1600.0 gal for load 5 to load 50 respectively. A reduction in the displacement and acceleration resulted due to an increase in cracking of concrete. The damping coefficients were calculated from the amplification factors which were compared with the measured value of the damping coefficientξ from the half-power method. The values of stiffness were directly calculated from the measured first resonant frequency and the mass. Then the maximum bending moment produced by the inertial force was calculated, and so were the dynamic bending stress and strain. This was then compared with the experimental strains.The strains and stresses from the SDOF model were on the lower side showing flexibility for higher periodic loads and a multi degree-of-freedom (MDOF)model became necessary to calculate the stresses and strains more accurately and a possible insight into the crack pattern.

Flexible Foundation Response

The flexible support specimen was tested on $9m^2$ soft soil having a very low G of 15~50 kg/cm^2 and ν of 0.40. An experimental procedure similar to the fixed base structure was followed. In case of a SDF, the foundation mass was neglected and only the overall, combined structural and soil stiffness and damping values were evaluated by the procedure outlined in the previous pages. A comparison of the results is shown in Table 2 and 3.

This was followed by a MDOF model supported by the lumped spring characteristics of the soft soil under the circular footing. The spring properties were those of the embedded circular footing using the elastic halfspace concepts already mentioned. The first mode in this case is also typical of the soil response and is horizontally displaced bending mode. These results revealed an interesting phenomenon of the footing loosing its embedment depth with increased amplitude of vibration. The structural properties were not found to be affected during such loading. However, the addition of the soil properties made the over all response quite linear with increased loading. The strains in this case were close to the experimentally observed values. New soil was used in each of the tests I, III, and V, which is also confirmed from the identification studies.

Table 2 Fixed Pier Summary

Counter Weight No.	Frequency (*Hz*)	Acceleration (*gal*)	Displacement (*cm*)	Exp. Damping Coefficient (%)	Calculated Strain ($\times 10^{-6}$)	Experimental Strain ($\times 10^{-6}$)
5	4.33	329	0.44	1.6	183	190
10	3.86	407	0.69	2.1	296	250
20	3.34	727	1.65	1.8	656	600
30	3.26	752	1.79	2.4	775	650
40	3.04	1030	2.84	2.0	1128	1270
50	2.93	1600	4.72	1.5	1913	1590
60	2.80	1350	4.36	1.9	1698	1680
70	2.70	1240	4.33	2.2	1687	2120
80	2.63	1290	4.75	2.3	1862	2290

Table 3 Flexible Pier Summary

Counter Weight No.	Frequency (*Hz*)	Acceleration (*gal*)	Displacement (*cm*)	Exp. Damping Coefficient (%)	Calculated Strain ($\times 10^{-6}$)	Shear Modulus (*MPa*)	Embedment (%)
5	2.58	34	0.12	5.6	42	2.4	100
10	2.38	65	0.29	4.9	66	2.4	50
30	2.14	142	0.79	5.5	124	2.4	20
90	2.07	272	1.49	8.1	207	2.4	0
10	2.07	49	0.29	5.0	117	2.4	100
30	1.84	117	0.89	4.9	230	2.4	50
90	1.58	224	2.28	5.3	406	1.8	0
10	1.93	40	0.27	5.2	128	2.4	100
30	1.74	87	0.73	5.9	224	2.4	50
90	1.53	230	2.49	4.8	515	1.8	0

CONCLUSIONS

1. The inclusion of material nonlinearity cannot be overlooked in a dynamic response of ductile structures, specially for reinforced concrete structures. The loading history and the number of cycles has a profound effect on the stiffness degradation and strength loss.
2. The pier acted as a hard spring for each load step earlier in the loading history and then gradually softened with increased loading.
3. The effect of the soft soil was evidently to isolate the structure and an attenuation of the response was observed. A simple elastic halfspace based lumped parametric approach was found to suffice the soil-structure model for identification studies.
4. A major effect of the reversed cyclic shear on plastic hinges is that sliding shear along the cracks leads to a loss of stiffness and energy dissipation. Significant pinching indicates that plastic hinges do not perform very well.

REFERENCES

Chen W. F. (1970). General Solution of Inelastic Beam-Column Problem, Jour. ASCE, Vol. 96, No. EM4, 421-441.

DebChaudhury A. (1985). Periodic Response of Yielding Oscillators, Jour. ASCE, Vol. 111, No. EM8, 977-994.

Gulkan P. and Sozen M. A. (1974). Inelastic Response of Reinforced Structures to Earthquake Motions, Jour. ACI, 604-610.

Jennings P. C. (1965). Earthquake Response of a Yielding Structure, Jour. ASCE, Vol. 91, No. EM4, 41-68.

Jiang Y. and Saiidi M. (1990). Four-Spring Element for Cyclic Response of R/C Columns, Jour. ASCE, Vol. 116, No. ST4, 1018-1029.

Kunnath S. K, Reinhorn A. M and Park Y. J. (1990). Analytical Modeling of Inelastic Seismic Response of R/C Structures, Jour. ASCE, Vol. 116, No. ST4, 996-1017.

Loh C. H. and Ho R. C. (1990). Seismic Damage Assesment Based on Different Hysteretic Rules, Earthquake Engineering and Structural Dynamics, Vol. 19, 753-771.

McNiven H. D. and Matzen V. C. (1978). A Mathematical Model to Predict the Inelastic Response of a Steel Frame: Establishment of Parameters from Shaking Table Experiments, Earthquake Engineering and Structural Dynamics, Vol. 6, 203-219.

Pais A. and Kausel E. (1988). Approximate Formulas for Dynamic Stiffness of Rigid Foundation, Soil Dynamics and Earthquake Engineering, Vol. 7, 213-229.

Veltsos A. S. and Meek J. W. (1974). Dynamic Behaviour of Building- Foundation Systems, Earthquake Engineering and Structural Dynamics, Vol. 3, 121-138.